Scaling properties of a simplified bouncer model and of Chirikov's standard map

2007 J. Phys. A: Math. Theor. 40 11467

(http://iopscience.iop.org/1751-8121/40/38/003)

IOP Publishing Journal of Physics A: Mathematical and Theoretical

J. Phys. A: Math. Theor. **40** (2007) 11467–11483 doi:10.1088/1751-8113/40/38/003

Scaling properties of a simplified bouncer model and of Chirikov's standard map

Denis Gouvêa Ladeira and Jafferson Kamphorst Leal da Silva

Departamento de Física, ICEx, Universidade Federal de Minas Gerais (UFMG), CP 702, 30.123-970 Belo Horizonte, MG, Brazil

E-mail: dgl@fisica.ufmg.br and jaff@fisica.ufmg.br

Received 17 April 2007, in final form 7 August 2007
Published 4 September 2007
Online at stacks.iop.org/JPhysA/40/11467

Abstract

Scaling properties of Chirikov's standard map are investigated by studying the average value of I^2, where I is the action variable, for initial conditions in (a) the stability island and (b) the chaotic component. Scaling behavior appears in three regimes, defined by the value of the control parameter K: (i) the integrable to non-integrable transition ($K \approx 0$) and $K < K_c$ ($K_c \approx 0.9716$); (ii) the transition from limited to unlimited growth of I^2, $K \gtrsim K_c$; (iii) the regime of strong nonlinearity, $K \gg K_c$. Our scaling results are also applicable to Pustylnikov's bouncer model, since it is globally equivalent to the standard map. We also describe the scaling properties of a stochastic version of the standard map, which exhibits unlimited growth of I^2 even for small values of K.

PACS numbers: 05.45.−a, 05.45.Pq, 05.45.Tp

(Some figures in this article are in colour only in the electronic version)

1. Introduction

In an attempt to understand the generation of cosmic rays, Fermi [1] proposed a mechanism in which charged particles are accelerated by time-dependent magnetic fields. Since this seminal work, the original model has been modified and investigated in the context of diverse applications. In the Fermi–Ulam model [2, 3] for example, a particle bounces between two rigid walls, one of which oscillates while the other is fixed. Another version of Fermi's model, in which a bouncing ball, under a gravitational acceleration g, strikes an oscillating platform, was introduced by Pustylnikov [4]. This model, also known as a bouncer model, shows unlimited energy growth for certain parameter and initial condition values [4, 5]. Lichtenberg [6] showed that Pustylnikov's bouncer model is equivalent, under a suitable transformation of variables, to the standard map introduced by Chirikov [7]. The quantum versions of the Fermi–Ulam and bouncer models have also been investigated [8–11]. These one-dimensional

models also allow direct comparison of theoretical predictions with experimental results [12, 13]. A recent review [5] covering all these topics was recently published.

The standard map is a dynamical system in the pair of variables I (action) and θ (the conjugate angle variable). The nonlinearity of the dynamics is controlled by a parameter K. If K is small enough, the phase space is characterized by a mixed structure, composed of KAM (Kolmogorov–Arnold–Moser) islands, regions of chaotic motion and spanning curves, which limit the orbits in the phase space. Consistent with the KAM theorem, however, above a critical value $K_c \approx 0.9716$, all the spanning curves of the standard map are destroyed. Thus for $K > K_c$ the quantity I^2 can grow, on average, without limit. (Unlimited growth of I^2 corresponds to Fermi acceleration in Pustylnikov's bouncer model.) Given the equivalence between the bouncer model and the standard map, it is natural to regard I^2 as the dimensionless particle energy. Since the scaling approach is a useful formalism for characterizing asymptotic properties, we study here the scaling properties of the energy in the standard map for regular and chaotic initial conditions.

Nonlinear systems such as the Fermi–Ulam model [14–16], time-dependent potential wells [17–19] and, recently, a version of a waveguide [20] are examples of dynamical models whose scaling properties have been investigated near the integrable to non-integrable transition. It is interesting to note that the average quantities characterizing the chaotic low energy regions of these models have the same exponents. So, it is legitimate to ask if Pustylnikov's bouncer model has also the same exponents near this transition. Here, we investigate the scaling features of the standard map in three regimes, characterized by different ranges of the control parameter K, namely (i) the transition from integrable to non-integrable ($K \approx 0$) and $K < K_c$, (ii) the transition from limited orbits in phase space to unlimited energy growth, in the regime of intermediate nonlinearity, $K \gtrsim K_c$, and (iii) the strongly nonlinear regime, $K \gg K_c$. We also derive analytically the scaling exponents of a stochastic version of the standard map, which exhibits, even for small values of K, unlimited growth of the variable I^2.

The paper is organized as follows. In section 2 we describe Pustylnikov's bouncer model and, briefly, present the equivalence between the bouncer model and the standard map, due to Lichenberg, and define the average quantities I^2 and $\overline{I^2}$. In section 3, we discuss the scaling description in the limit of small K. In sections 4 and 5 we turn, respectively, to the scaling properties of I^2 when $K \gtrsim K_c$ and $K \gg K_c$. In section 6 we analyze a stochastic version of the standard map, whose scaling relations are derived analytically. Finally we present, in section 7, a summary of the results and our conclusions.

2. Pustylnikov's bouncer model and the standard map

The bouncer model consists of a classical particle moving in one dimension and subject to gravitational acceleration g, which makes collisions with an oscillating platform. The position y of this platform oscillates with amplitude ϵ and frequency ω, i.e. $y = \epsilon \cos(\omega t + \phi_0)$, where ϕ_0 is an initial phase and t is the time. In the *simplified bouncer model*, the platform is assumed fixed but the momentum transfer occurs as if it were moving. If v_n is the velocity of the particle and $\omega t_n + \phi_0$ is the phase of the oscillating wall immediately after the nth impact, then, in terms of the new and dimensionless variables $V_n = \omega v_n / g$ and $\phi_n = \omega t_n + \phi_0$, the dynamics of the simplified bouncer model is given by the two-dimensional map:

$$T : \begin{cases} V_{n+1} = |V_n - 2\varepsilon \sin \phi_{n+1}|, \\ \phi_{n+1} = \phi_n + 2V_n \mod 2\pi, \end{cases}$$

where the dimensionless parameter $\varepsilon = \epsilon \omega^2 / g$ is the ratio of the maximum wall acceleration to the gravitational acceleration. The absolute value is required here because negative velocities

are forbidden in the simplified version. Lichtenberg [6] showed that under the transformation of variables $I_n = 2V_n$, $K = 4\varepsilon$ and $\theta_n = \phi_{n+1} + \pi$, Pustylnikov's bouncer model is globally equivalent to the standard map with action I and conjugate angle θ. The standard map is defined by

$$T_s : \begin{cases} I_{n+1} = I_n + K \sin\theta_n, \\ \theta_{n+1} = \theta_n + I_{n+1} \mod 2\pi. \end{cases} \tag{1}$$

Although the simplified bouncer model differs from the standard map (the evolution of V_n involves the absolute value), the principal dynamic properties of the standard map, such as the transitions from integrable to non-integrable motion and from bounded to unbounded values of I, are not affected by introducing the absolute value. (The latter affects only the small-I regime.) We may therefore gain insight from the scaling properties of the standard map. Given the relation between variables I and V, it follows that I^2 is proportional to the dimensionless particle energy in the bouncer model.

For small values of K ($K \ll K_c$), the phase space of the standard map basically consists of elliptic fixed points surrounded by islands of regular motion. The chaotic regions are very small and occur near separatrices that are isolated. As long as K is larger than K_c, the last spanning curve (separatrix) between the period-1 and period-2 islands disappears and the system presents a global chaotic component. Now, initial conditions in the chaotic sea present unlimited average energy growth due to the diffusion in the stochastic region. These points present Fermi acceleration according to Ulam's point of view. When $K \gg K_c$, the chaotic component surrounds small regions of regular motion. It is worth mentioning that the size of these regions decreases rapidly as K grows. Since we want to study the bouncer model, we consider that the action is not modulo 2π. However, for the standard map, it is natural to define I as modulo 2π (see equation (1) for θ_{n+1}). This implies that fixed point equations ($K \sin(\theta) = 2\pi l$, $I = 2\pi m$) admit windows of values for successively large values of K in which the solutions are stable. This discussion can be generalized to $m > 1$ fixed points. However, for the standard map defined in equation (1) these periodic orbits do not exist and the windows of the parameter where stable motion was observed now furnish the values of K for which the action grows unlimitedly. The period-1 orbits, for example, are replaced by *accelerator modes* characterized by unlimited growth of the action as $I_n = I + 2\pi ln$. Because it is not a stable motion, this kind of movement is usually called as *regular*. It follows that the ensemble of these orbits and their neighborhoods also presents unlimited growth of the energy (Fermi acceleration in the sense of Pustylnikov) [2, 4–7, 11, 21].

Prior to discussing the scaling properties of the standard map, it is convenient to define the average quantities of interest. We define the average squared action variable over the orbit associated with an initial condition j as

$$\left\langle I^2_{n,j} \right\rangle = \frac{1}{n+1} \sum_{i=0}^{n} I^2_{i,j}, \tag{2}$$

where i refers to the ith iteration of the map. We then define an average over M independent realizations of the map, characterized by randomly chosen values of θ_0:

$$I^2(n, K, I_0) = \frac{1}{M} \sum_{j=1}^{M} \left\langle I^2_{n,j} \right\rangle. \tag{3}$$

We are also interested in the ensemble average of the energy evaluated at iteration n, namely

$$\overline{I^2}(n, K, I_0) = \frac{1}{M} \sum_{j=1}^{M} I^2_{n,j}. \tag{4}$$

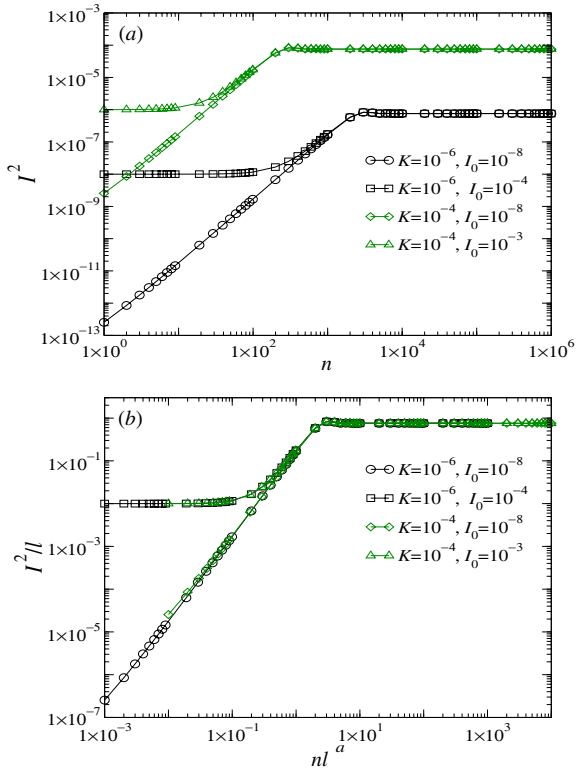

Figure 1. (*a*) I^2 versus n for the standard map in the weakly nonlinear regime, for control parameter K and initial values I_0 as indicated. The results represent averages over $M = 10^3$ realizations. (*b*) Scaling plot, I^2/l versus nl^a, where $l = K^{-1/b}$, demonstrating collapse of the curves in (*a*) onto universal curves. The initial conditions are inside a stability island.

In this work, we study the scaling properties of I^2 and $\overline{I^2}$ that are related to corresponding particle energy averages in Pustylnikov's bouncer model.

3. Weakly nonlinear regime

Let us first discuss scaling in the weakly nonlinear regime. As is clear from equation (1), if $K \approx 0$ the system is near the integrable to non-integrable transition. In this regime, the period-1 and -2 fixed points are separated by invariant spanning curves, and we can have two kinds of initial conditions: (a) points inside a stability island and (b) points in the chaotic component near the first separatrix. Let us first study case (a).

For $I_0 \ll K$, I^2 grows with n, but saturates at a finite limiting value for $n \gg 1$, as is shown in figure 1(*a*). We can define a crossover value n_x, at which I^2 switches from the growth regime to its limiting value.

For $I_0 \gg K$, (figure 1(*a*)), we find $I^2 \approx I_0^2$, for small n; I^2 subsequently grows and approaches the behavior observed for $I_0 \ll K$. Thus, the asymptotic value of I^2 is independent of its initial value. In the case $I_0 \gg K$, we can identify two crossover values, n'_x and n''_x, at which the behavior of I^2 changes. The first, n'_x, characterizes the change from the initial

regime of constant I^2 to the growth regime; the second, n_x'', marks the change from the growth regime to saturation. Moreover, for a given value of K, figure 1(*a*) shows that $n_x'' \approx n_x$.

In the limit $I_0 \approx 0$, we can describe, for $n \ll n_x$, the initial growth of I^2 as

$$I^2(n, K, 0) \propto n^\alpha K^\beta, \tag{5}$$

where α is the growth exponent and β is the exponent that governs the K-dependence for small values of n. In the limit $n \gg n_x$, for which the I^2 curves saturate, we can write

$$I^2_{\text{sat}} \propto K^\gamma, \tag{6}$$

where γ is the saturation exponent. Moreover, we can define the dynamic exponent z by expressing the crossover iteration number n_x as a function of the parameter K as

$$n_x \propto K^z. \tag{7}$$

We are now ready to formally express the scaling relations for I^2. Since I^2 is a function of n, K and I_0, we can write

$$I^2(n, K, I_0) = l I^2(l^a n, l^b K, l^c I_0), \tag{8}$$

where l is the scale factor and a, b and c are scaling exponents. Choosing $l = K^{-1/b}$, the above equation can be written as

$$I^2(n, K, I_0) = K^{-1/b} f(K^{-a/b} n, K^{-c/b} I_0), \tag{9}$$

where $f = I^2(K^{-a/b} n, 1, K^{-c/b} I_0)$ is assumed to be constant for $n \gg n_x$. Then, comparing equations (6) and (9), we observe that $\gamma = -1/b$. Setting $l = n^{-1/a}$, equation (8) implies

$$\begin{aligned} I^2(n, K, I_0) &= n^{-1/a} g(n^{-b/a} K, n^{-c/a} I_0) \\ &= n^{-(1+by)/a} K^y h(n^{-c/a} I_0), \end{aligned} \tag{10}$$

where $g = I^2(1, n^{-b/a} K, n^{-c/a} I_0)$. In the limit $I_0 \ll K$ the function h is assumed to be constant, and for small values of n, we can conclude, from equations (5) and (10), that $\alpha = -(1 + by)/a$ and $\beta = y$. The exponent c can be obtained from the relation $I^2/K = \text{constant}$. Defining $K' = l^b K$ and $I_0' = l^c I_0$ we can write $I^2/K = I'^2/K' = (l^c I_0)^2/l^b K$ and, therefore, obtain $c = b/2$. From equation (9), the crossover n_x scales with K as

$$n_x \approx K^{a/b}. \tag{11}$$

From this last equation and equation (7), we obtain $z = a/b$.

We determine α via a fit to the initial growth regime of each I^2 curve; using K in the interval $[10^{-6}, 10^{-2}]$, we obtain $\alpha = 1.91 \pm 0.01$. The exponent β in equation (5) gives the dependence of the initial growth of I^2 on K. Therefore, β can be determined by a best fit to the data for $n \ll n_x$, in a plot of I^2/n^α versus K on logarithmic scales. This procedure, shown in figure 2(*a*), yields $\beta = 2.012 \pm 0.005$.

The dynamic exponent z is similarly obtained from a fit to the data in a plot of n_x versus K; this furnishes $z = -0.505 \pm 0.006$, as is shown in figure 2(*b*). Knowing the values of exponents α, β and z, we can obtain the values of all other exponents. The scaling exponents are $a = 0.48 \pm 0.02$, $b = a/z = -0.95 \pm 0.05$ and $c = b/2 = -0.48 \pm 0.03$. The saturation exponent is $\gamma = -1/b = 1.06 \pm 0.06$. With these exponents, we can choose $l = K^{-1/b}$ and, applying the scale transformations $n \to n l^a$ and $I^2 \to I^2/l$, we obtain the collapse of the I^2 curves onto a universal one. These transformations are illustrated in figure 1(*b*), for both $I_0 \ll K$ and $I_0 \gg K$.

It is also possible to determine the initial growth of I^2 analytically for small θ_0 and $K \ll K_c$. Noting that $I_0 \approx 0$ for $nK \ll 1$, the sine in equation (1) can be expanded to the first order to yield $I_n \approx nK\theta_0$ or $I_n^2 \propto n^2 K^2$, describing the behavior of I^2 for $I_0 \ll K \ll K_c$.

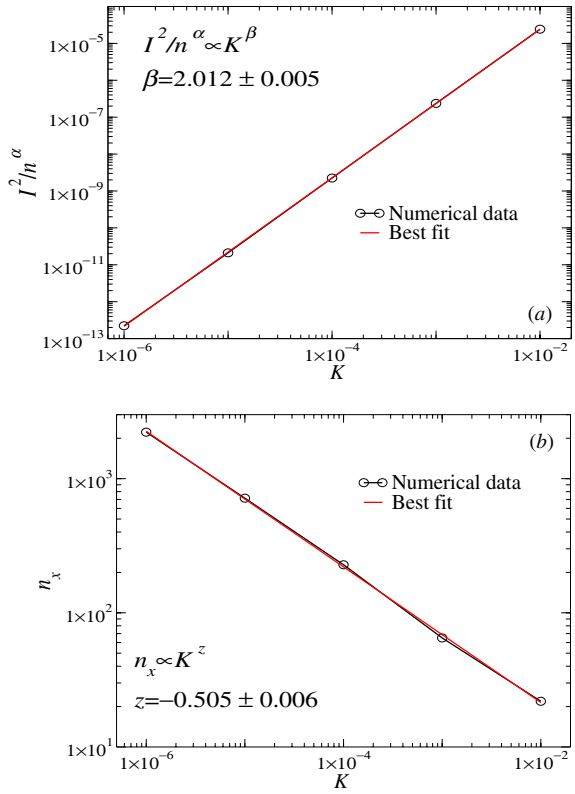

Figure 2. (*a*) Log–log plot of I^2/n^α versus K for $n \ll n_x$. A least-squares linear fit yields $\beta \approx 2$. (*b*) Crossover number n_x versus K. The best fit gives $z = -0.505 \pm 0.006$. The initial conditions are inside a stability island.

We also study the behavior of I^2 for the regular initial conditions when $K \in [0.1, 0.9]$. It turns out that I^2 shows a scaling behavior with the exponents a and b equal as the ones obtained for $K \approx 0$. However, the exponent c cannot be obtained because the regime $I_0 \gg K$ is not reachable.

To study the behavior of initial conditions in the chaotic region (case (b)), we must deal with the small size of this region. In fact for $K \approx 0$ it is very hard to observe numerically this region. Since the scaling behavior of I^2 for the initial conditions inside the stability island is valid for $K \in [10^{-6}, 0.9]$, it is legitimate to study the behavior of the chaotic points for $K \in [0.1, 0.9]$. In this interval for K, the chaotic region has enough separated points to allow good simulations. It is possible that the obtained scaling be valid for $K \approx 0$. From figure 3(*a*) and from a similar plot of the crossover, we obtain that $\gamma = 1.72 \pm 0.04$ and $z = -1.43 \pm 0.08$. Thus, it follows that the scaling exponents are $a = 0.83 \pm 0.06$ and $b = -0.58 \pm 0.01$. These exponents are used to collapse I^2 versus n curves onto a universal one, as is shown for a particular case in figure 3(*b*). We must observe that the collapse for small K is not very good because the chaotic region is very small and it furnishes only initial conditions that are all close to each other. To obtain the exponent c, we need that $I_0 \gg K$. This condition cannot be satisfied because K is too large and an appropriate I_0 would be above the saturation I_{sat}. We must also observe that we are not able to obtain the α exponent because the growth regime is very small (only one order of magnitude in the variable n).

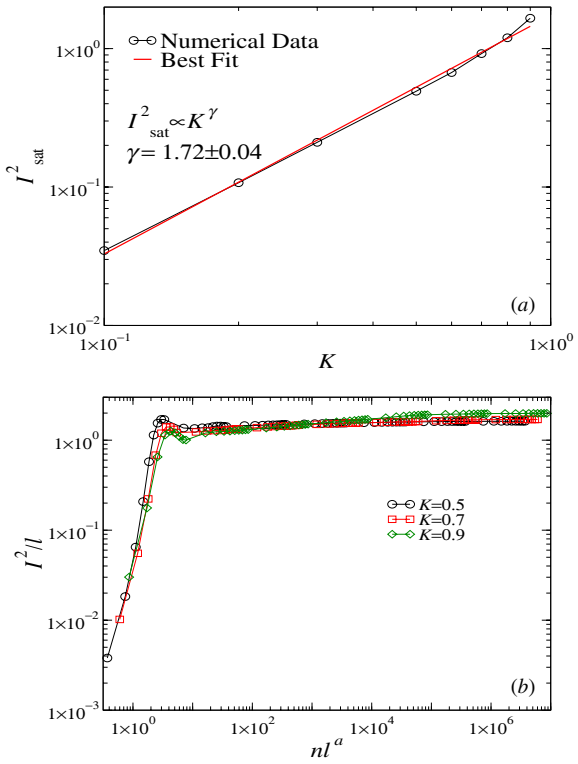

Figure 3. (*a*) Log–log plot of $I^2_{\rm sat}$ versus K. The initial conditions are near the first separatrix (chaotic region). A least-squares linear fit yields $\gamma = 1.72 \pm 0.04$. (*b*) Log–log scaling plot, I^2/l versus nl^a, where $l = K^{-1/b}$, demonstrating the collapse of two curves onto a universal one.

4. Moderately nonlinear regime

The moderately nonlinear regime corresponds to $K \gtrsim K_c$. ($K_c \simeq 0.9716$ is the critical value, at which the last spanning curve between the period-1 and period-2 fixed points is destroyed.) For initial points inside the first island, I^2 grows for small n and reaches a constant value. On the other hand, for initial points in the chaotic component, this regime marks the transition from saturation to unlimited growth of I^2 due to diffusion in the stochastic region [11]. We define $K_r = K - K_c$ and study the scaling properties of I^2 for $K_r \gtrsim 0$. In this regime, I^2 grows slowly for small n and crosses over to a more rapid growth for $n > n_x$ (figure 4(*a*)). Evidently, I^2 grows without limit as $n \to \infty$.

We find that the crossover iteration number, n_x, diverges as $K_r \to 0$, following

$$n_x \propto K_r^z. \tag{12}$$

A least-squares best fit to the data (figure 5(*a*)) yields $z = -2.99 \pm 0.09$.

In the limit $n \gg n_x$, the growth of I^2 is described by

$$I^2 \propto n^{\alpha} K_r^{\beta}. \tag{13}$$

Fitting the data (an average over 11 realizations) in this regime, with $K_r \in [8.4 \times 10^{-3}, 1.284 \times 10^{-1}]$ we obtain $\alpha = 0.99 \pm 0.03 \approx 1$. The value of β can be obtained directly by fitting I^2/n versus K_r on the log scale; this furnishes $\beta = 3.06 \pm 0.05 \approx 3$ (figure 5(*b*)).

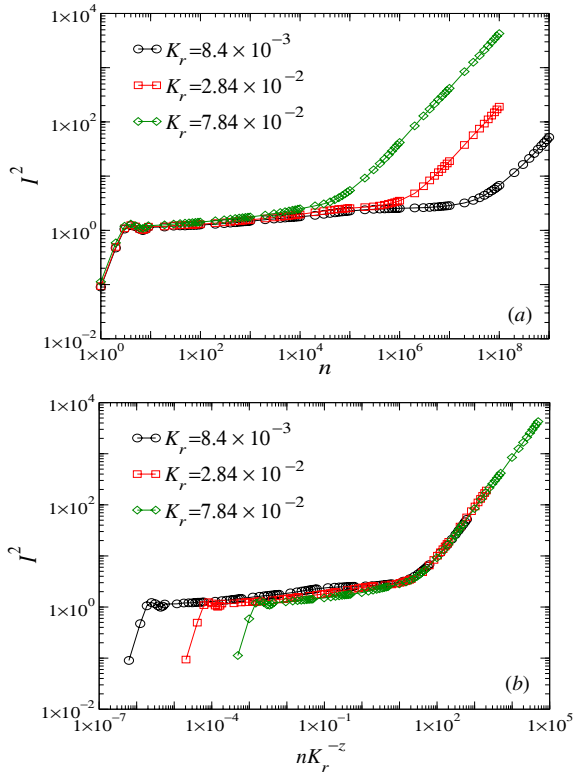

Figure 4. (*a*) I^2 versus n for $K \gtrsim K_c$, when the initial conditions belong to the chaotic component. (The data represent averages over 10^3 independent realizations.) (*b*) Collapse of the I^2 data shown in (*a*) onto a universal curve.

Thus the asymptotic growth of I^2, for $K \gtrsim K_c$, is well described by $I^2 \propto nK_r^3$. Formally, the scaling relation of I^2 in the regime $K \gtrsim K_c$ can be written as

$$I^2(n, K_r) = lI^2(l^a n, l^b K_r). \tag{14}$$

Letting $l = K_r^{-1/b}$, this becomes

$$I^2(n, K_r) = K_r^{-1/b} f\left(K_r^{-a/b} n\right), \tag{15}$$

which in turn implies that the crossover number follows $n_x \propto K_r^{a/b}$. Thus, from equation (12), we have $z = a/b$. Equation (15) can be written as

$$I^2(n, K_r) \propto K_r^{-1/b}\left(K_r^{-a/b} n\right)^x. \tag{16}$$

Turning to the limit $n \gg n_x$ we find, from the above equation and equation (13), that $x = \alpha$ and $-1/b = z\alpha + \beta$. Now letting $l = n^{-1/a}$, equation (14) yields

$$\begin{aligned} I^2(n, K_r) &= n^{-1/a} f(n^{-b/a} K_r) \\ &= n^{-1/a}(n^{-b/a} K_r)^y \end{aligned} \tag{17}$$

and, from equation (13), we have that $y = \beta$ and $-1/a = \alpha + \beta/z$. Since $\alpha \approx 1, z \approx -3$ and $\beta \approx 3$, we obtain that $-1/a = \alpha + \beta/z = 0$ and $-1/b = z\alpha + \beta = 0$. Therefore the exponents a and b diverge but their ratio is finite, since $z = a/b \approx -3$. Therefore if we choose

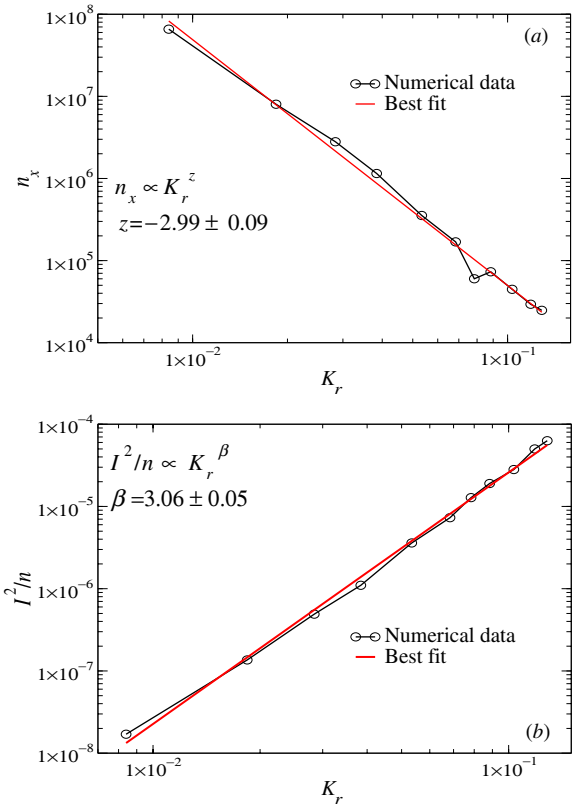

Figure 5. (*a*) Crossover iteration number n_x versus $K_r = K - K_c$ for $K \gtrsim K_c$. The best fit to the data furnishes $z = -2.99 \pm 0.09$. (*b*) I^2/n versus K_r. The best fit gives $\beta = 3.06 \pm 0.05$.

$l = K_r^{-1/b}$ we have $l \approx 1$, $nl^a = nK_r^{-z}$ and the rescaled I^2 data collapse in the large-n limit, as is shown in figure 4(*b*).

Figure 6 shows the behavior of $\overline{I^2}$ (see equation (4)). Except for initial oscillations, the overall behavior is the same as that of I^2 (see figure 4). In particular, the scaling exponents for the two kinds of average are the same.

5. Strongly nonlinear regime

The third scaling regime is characterized by $K \gg K_c$. In this limit, all the spanning curves between the period-1 and period-2 fixed points have disappeared and the stochastic component spreads all over the phase space. Moreover, unlimited growth of I is observed in some regions of regular motion in the phase space for arbitrary values of K [4]. The condition $4s\pi \leqslant K < 4\sqrt{1+(s\pi)^2}$, where $s = l/2$ and l is an integer, furnishes the intervals of K for which the most simple kind of regular growth of the action is observed [5, 7, 21]. For each of these regular regions there is a fixed value of θ for which the variable action increases unlimitedly as $I_n = 2\pi m + 2\pi ln$, m being an integer. Orbits characterized by unlimited growth of the action are also observed near enough to these trajectories. The first nontrivial motion characterized by a regular increase of the action is obtained for $l = 1$ and $m = 1$. Thus, the

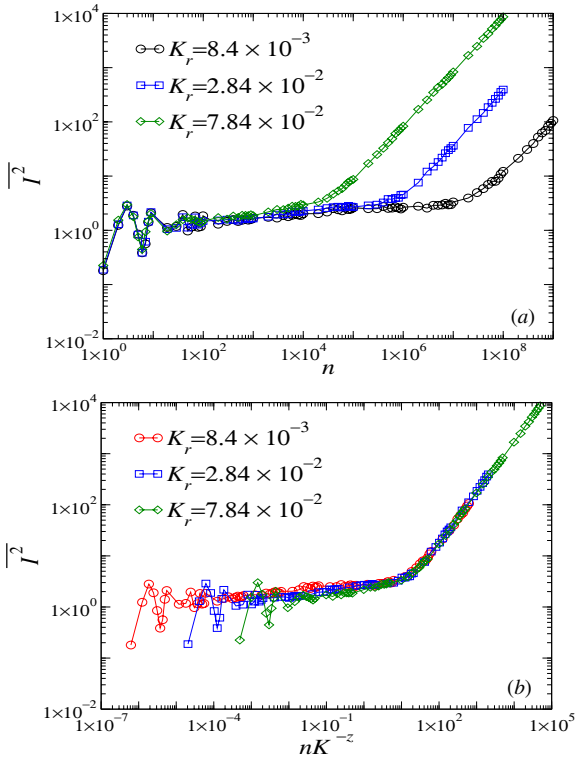

Figure 6. (*a*) $\overline{I^2}$ versus n for $K \gtrsim K_c$, when the initial conditions belong to the chaotic component. (The data represent averages over 10^3 independent realizations.) (*b*) Collapse of the I^2 data shown in (*a*) onto a universal curve.

first accelerator mode occurs for $K > 2\pi$. Similarly, accelerator modes of regular motion are observed for arbitrary values of K. Windows of K for other kinds of regular motion are also observed for arbitrary values of the parameter. Although there is a large number of such regions of regular motion, the size of these accelerator modes decreases rapidly as K grows [7]. Now an unlimited growth of the energy appears for initial points inside (a) the stochastic component and (b) the regions of regular dynamics.

Performing averages over 10^3 realizations, characterized by randomly chosen values of θ_0 and different values of I_0 belonging to the chaotic component, we again considered the average quantity I^2 defined in equation (3). Figure 7(*a*) shows I^2 for two K values satisfying $K \gg K_c$, for both $I_0 \ll K$ and $I_0 \gg K$. If $I_0 \ll K$, then I^2 grows in a power-law fashion and does not depend on the initial value I_0. Considering first the case $I_0 \ll K$, we have

$$I^2 \propto n^{\alpha} K^{\beta}, \tag{18}$$

where α is the growth exponent and β gives the dependence of I^2 on K. Performing nonlinear fits for values of $K \in [10^1, 10^5]$ we obtain $\alpha = 0.999 \pm 0.001 \approx 1$ and, from a plot of I^2/n versus K, we find $\beta = 2.02 \pm 0.02 \approx 2$ (figure 8(*a*)).

Turning to the regime $I_0 \gg K$, we see that there is, for each I^2 curve, a crossover number, $n = n_x$, prior to which I^2 is essentially constant, $\left(I^2 \approx I_0^2\right)$, and after which I^2 grows. We also note that, for large values of n, the value of I^2 does not depend on I_0, for both $I_0 \ll K$

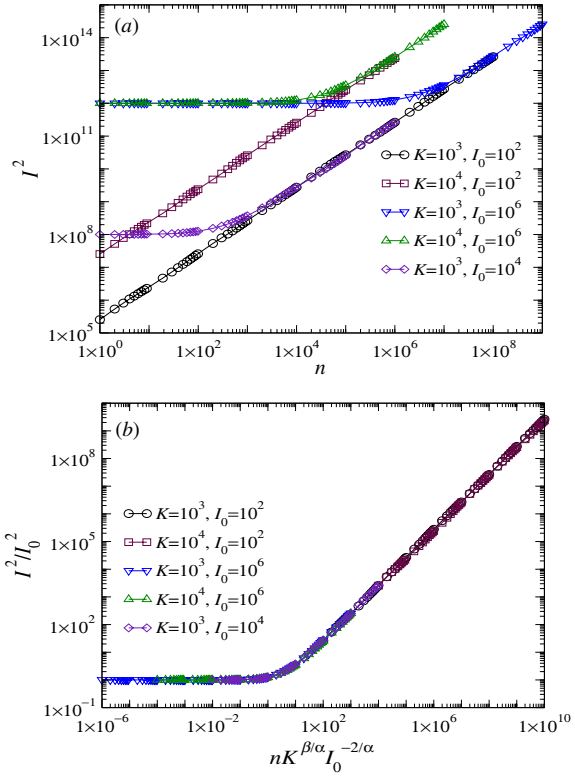

Figure 7. (*a*) Log–log plot of I^2 versus n for $K \gg K_c$. (*b*) Collapse of the data shown in (*a*) under the scaling transformation.

and $I_0 \gg K$. As is evident in figure 7(*a*), the crossover number, n_x, depends on both I_0 and K. We may write

$$n_x \propto I_0^{z_1} K^{z_2}, \tag{19}$$

where z_1 and z_2 are dynamic exponents. Plotting n_x as a function of I_0, we obtain $z_1 = 1.98 \pm 0.02$ from the best fit. Similarly, a plot of n_x versus K furnishes $z_2 = -1.98 \pm 0.02$ (figures 8(*b*), (*c*)). In figure 8(*b*), $K = 10^3$ is the same in all the studies, while in figure 8(*c*), I_0 is fixed at $I_0 = 10^6$.

It is useful to define a scaling variable nK^x, in terms of which we shall describe the behavior of I^2. Given the values of α and β, the exponent x can be determined from equation (18) and the scaling properties of I^2. Thus, considering I^2 as a function of nK^x and I_0, we have

$$I^2(nK^x, I_0) = lI^2(l^d nK^x, l^e I_0), \tag{20}$$

where d and e are scaling exponents and l is a scaling factor. Setting $l = (nK^x)^{-1/d}$ yields

$$\begin{aligned} I^2(nK^x, I_0) &= (nK^x)^{-1/d} f((nK^x)^{-e/d} I_0) \\ &\propto (nK^x)^{-1/d} [(nK^x)^{-e/d} I_0]^y. \end{aligned} \tag{21}$$

For $n \gg n_x$ we see that I^2 does not depend on I_0 and, therefore, $y = 0$ in the above equation. Thus, from equation (18), we observe that $-1/d = \alpha$ and $-x/d = \alpha x = \beta$. For $n \ll n_x$ we

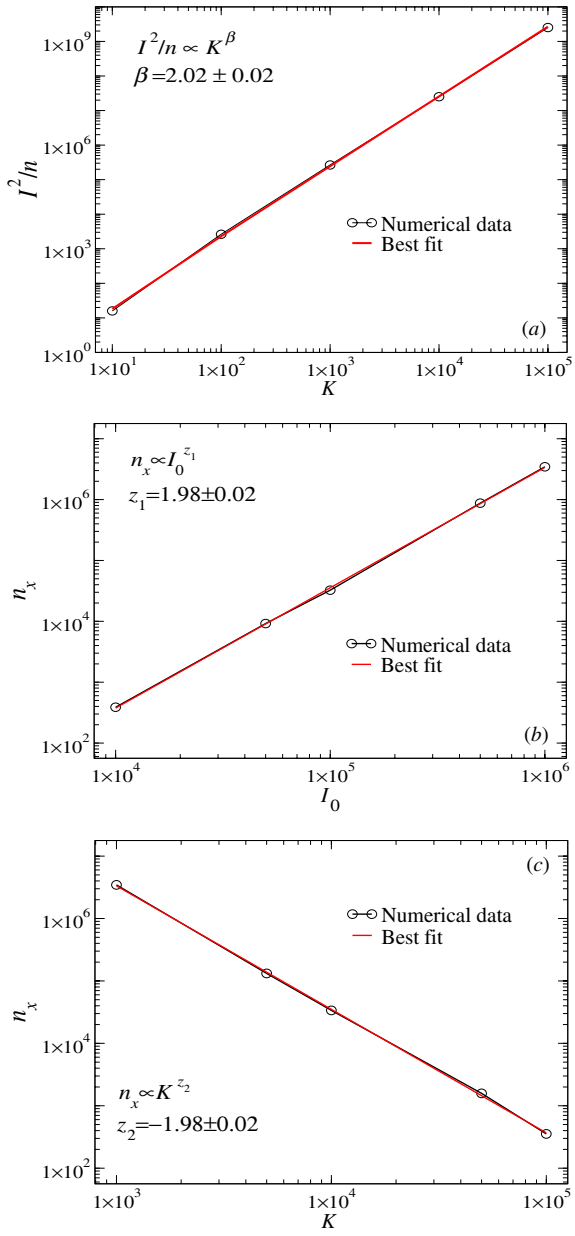

Figure 8. Log–log plot of I^2/n versus K. The best fit to the data furnishes $\beta = 2.02 \pm 0.02$. (*b*), (*c*) Plots of the crossover number n_x as a function of I_0 and K. In (*b*) $K = 10^3$; in (*c*) $I_0 = 10^6$.

have that, if $I_0 \ll K$, then $y = 0$ in equation (21). However, if $I_0 \gg K$, then $y = 2$ and, since in this limit I^2 does not depend on n or K, we also have that $e = -1/2$. As $\alpha = 0.999 \pm 0.001$ and $\beta = 2.02 \pm 0.02$, we have $x = \beta/\alpha = 2.02 \pm 0.02$ and $d = -1/\alpha = -1.001 \pm 0.001$. Letting $l = I_0^{-1/e}$, equation (20) becomes

$$I^2(nK^x, I_0) = I_0^{-1/e} g\left(I_0^{-d/e} n K^x\right). \tag{22}$$

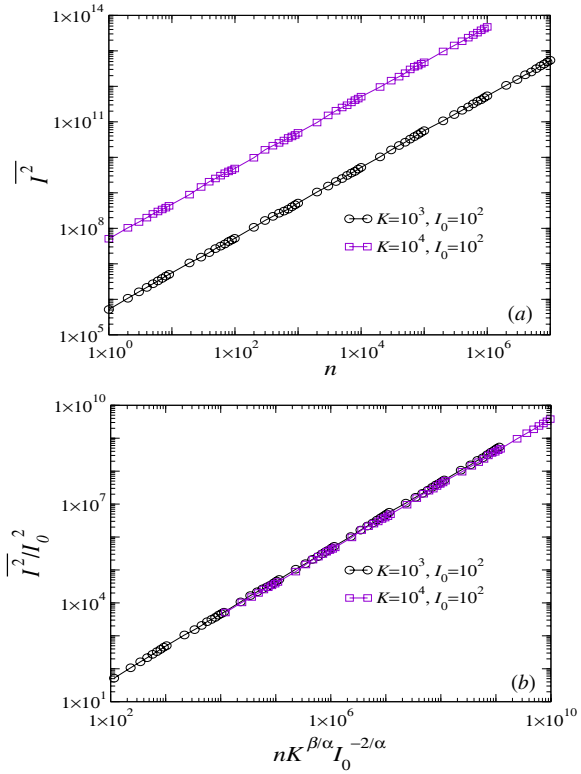

Figure 9. (*a*) Log–log plot of $\overline{I^2}$ for $K \gg K_c$ and (*b*) the collapse of the curves in (*a*) onto a universal curve is obtained with the same exponents of collapse for I^2.

From this relation, we have $n_x \approx I_0^{d/e}/K^x$. In terms of the exponents α and β, this can be written as

$$n_x \approx \left(\frac{I_0^2}{K^\beta}\right)^{1/\alpha}. \tag{23}$$

Since $2/\alpha = 2.002 \pm 0.002$ and $\beta/\alpha = 2.02 \pm 0.02$, we can compare equations (19) and (23) and, considering the uncertainties, we have that $z_1 \approx 2/\alpha$ and $z_2 \approx -\beta/\alpha$ respectively. Thus, performing the scaling transformations $I^2 \to I^2/l$ and $n \to l^{-1/\alpha} n K^{\beta/\alpha}$, with $l = I_0^{-1/e} = I_0^2$, we collapse all the I^2 curves, as is shown in figure 7(*b*).

The behavior of $\overline{I^2}$ for two values of K is displayed in figure 9(*a*). The collapse of these curves onto a universal curve, as is displayed in figure 9(*b*), by using the same set of exponents of the collapse for I^2 (see figure 7) shows that both averages have the same scaling behavior.

6. Stochastic version of the standard map

Study of stochastic versions of Fermi-like models began with Hammersley's work [22] on the Fermi–Ulam model, in which a bouncing particle is confined between two walls, one of which is fixed and the other moving randomly. In the stochastic Fermi–Ulam model, the average particle energy grows without limit. Recently, Karlis *et al* [23] studied a version of the

Fermi–Ulam model with stochastic momentum transfer between the particle and either wall. In this section we study a map in which the angle θ_n does not evolve as in equation (1), but is given, independently at each iteration by a random variable uniformly distributed on $[0, 2\pi)$. This random shift can be interpreted as an irregular interaction of a particle with a thermal bath. For a given realization j, we evaluate the action variable according to the map (1), with θ_n random, yielding

$$I_{n,j} = I_{0,j} + K \sum_{k=0}^{n-1} \sin\theta_k. \tag{24}$$

Evaluating the mean-square action variable, we have

$$\left\langle I_{n,j}^2 \right\rangle = \frac{1}{n+1}\left[(n+1)I_0^2 + 2KI_0 \sum_{k=0}^{n-1}(n-k)\sin\theta_k + K^2 \sum_{k=0}^{n-1}\left(\sum_{k'=0}^{k}\sin\theta_{k'}\right)^2\right]. \tag{25}$$

Now consider the average of I^2 over a sample of M realizations, as defined in equation (3). Since the θ values are independent and uniformly distributed on $[0, 2\pi)$, the mean of $\sin\theta_k$ is zero while that of $\sin^2\theta_k$ is $1/2$. Thus, imposing the same initial value I_0 for all M realizations, we have

$$I^2 = I_0^2 + \frac{K^2}{4}n. \tag{26}$$

As before, $I^2 \propto n$ corresponds to unlimited energy growth, or Fermi acceleration, in Pustylnikov's bouncer model. Figure 10(a) shows I^2 as given by equation (26) for several values of K and I_0. For $I_0 \gg K_c$, I^2 is essentially constant for $n < n_x$, and approaches the corresponding I^2 curve (for $I_0 \ll K_c$ and the same value of K), thereafter. It is worth mentioning that the numerical results agree very well with the analytical ones.

For $n \ll n_x$, equation (26) implies $I^2 \approx I_0^2$. In the opposite limit ($n \gg n_x$), we have $I^2 \approx K^2 n/4$. Therefore, the crossover number n_x obeys

$$n_x \approx 4\left(\frac{I_0}{K}\right)^2. \tag{27}$$

In terms of the scaling variable nK^2, the scaling function for I^2 is formally written as

$$I^2(nK^2, I_0) = lI^2(l^d nK^2, l^e I_0). \tag{28}$$

Setting $l = (nK^2)^{-1/d}$, the above equation can be rewritten as

$$I^2(nK^2, I_0) = (nK^2)^{-1/d} f((nK^2)^{-e/d} I_0). \tag{29}$$

For $n \gg n_x$, the function $f = I^2(1, (nK^2)^{-e/d} I_0)$ is constant and, from equation (26), we have $-1/d = 1$ or $d = -1$. Letting $l = I_0^{-1/e}$, equation (28) implies

$$I^2(nK^2, I_0) = I_0^{-1/e} g\left(I_0^{-d/e} nK^2\right). \tag{30}$$

From this relation, we have

$$n_x \approx I_0^{d/e}/K^2. \tag{31}$$

This relation and equation (27) therefore imply $d/e = 2$ and, thus, $e = -1/2$. Figure 10(b) confirms that, by appropriate scaling transformations, the data for I^2 displayed in figure 10(a) collapse onto a single, universal curve.

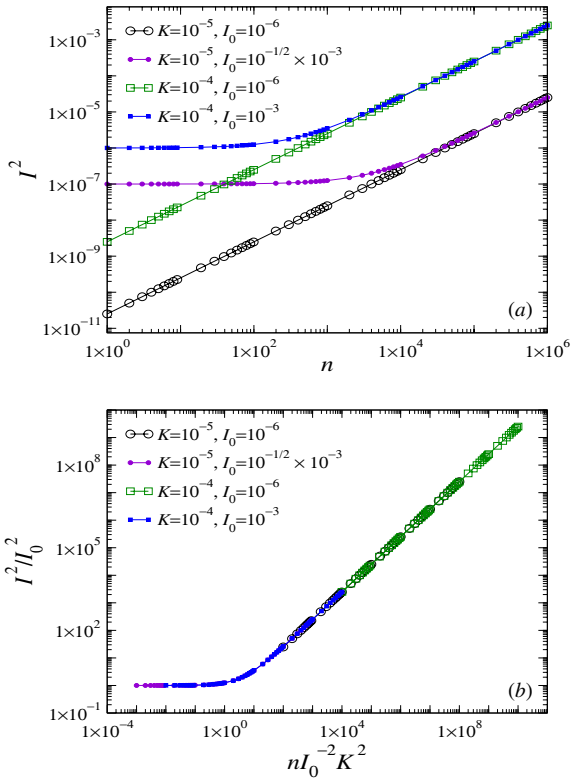

Figure 10. I^2 versus n for the stochastic standard map. (a) Analytical result, equation (26), for K and I_0 as indicated and (b) data collapse under scaling transformation.

7. Summary and conclusions

We have investigated the scaling properties of Chirikov's standard map [7]. Since, as shown by Lichenberg [6], the standard map is equivalent to Pustylnikov's bouncer model [4], our results are applicable to the latter as well. We analyzed the energy by taking two kinds of averages: (i) an average only over the ensemble of initial $\theta(\overline{I^2})$ and (ii) an average along an orbit followed by the ensemble average (I^2). $\overline{I^2}$ and I^2 have the same scaling behavior.

For $K \approx 0$ we studied the scaling properties of I^2 near the integrable to non-integrable transition for initial points in the stability island. This scaling description is valid even for $K \in [10^{-6}, 0.9]$. When the initial conditions were near the first separatrix (chaotic component), we were able to obtain a scaling description only for $K \in [0.1, 0.9]$. When $K \approx 0$ we had numerical problems related to the small size of the chaotic region. However, it is possible that the obtained exponents be valid in this limit. We emphasize that all obtained exponents are different from those characterizing the integrable to non-integrable transition of the Fermi–Ulam model. The different sets of exponents reflect their different transitions. For low energies, the phase space of the Fermi–Ulam model is essentially chaotic while the standard map presents a stability island with a chaotic layer.

For $K \gtrsim K_c$ we described, by scaling analyses, the transition from limited to unlimited growth of I^2 for initial points in the chaotic component, or transition to unbounded energy gain, the so-called Fermi acceleration phenomena, in Pustylnikov's bouncer model. We also

Table 1. Summary of the scaling description of the standard map. Note that $K^{\dagger}$ is given by $K^{\dagger} = K_r$ for $K \gtrsim K_c$ and $K^{\dagger} = K$ for the other cases. The initial conditions belong to regular motion (first case) and to the chaotic component (other cases).

Regime	Scaling variables	Scaling exponents	Growth regime $I^2 \propto n^{\alpha} K^{\dagger\beta}$
$K < K_c$	n	$a = 0.48(2)$	$n \ll n_x$
or	K	$b = -0.95(5)$	$\alpha = 1.91(1)$
$K \approx 0$	I_0	$c = -0.48(3)$	$\beta = 2.012(5)$
(reg. i.c.)			
$K < K_c$	n	$a = 0.83 \pm 0.06$	
	K	$b = -0.58 \pm 0.01$	
$K \gtrsim K_c$	n		$n \gg n_x$
	$K_r = K - K_c$	$a/b = -2.99(9)$	$\alpha = 0.99(3)$
			$\beta = 3.06(5)$
$K \gg K_c$	$nK^{\beta/\alpha}$	$d = -1.001(1)$	$n \gg n_x$
	I_0	$e = -1/2$	$\alpha = 0.999(1)$
			$\beta = 2.02(2)$
Stochastic	nK^2	$d = -1$	$n \gg n_x$
version	I_0	$e = -1/2$	$\alpha = 1$
			$\beta = 2$

derived the scaling descriptions of the standard map for the regime of strong nonlinearity, $K \gg K_c$. Moreover, we analyzed a stochastic version of the standard map, in which the angle variable, θ, is random. In this last version the variable I^2 exhibits unlimited growth, even for $K \approx 0$. In terms of the variables of the bouncer model, this means that the particle experiences unbounded energy gain [22]. In table 1, we summarize the main results of the scaling description. As is shown in the final column of table 1, we find that for regular orbits in the limit of weak nonlinearity and for small n, $I^2 \propto n^2K^2$. For chaotic orbits, with $K \gtrsim K_c$, we showed for large n that $I^2 \propto nK_r^3$, where $K_r = K - K_c$, while in the limit of strong nonlinearity, $K \gg K_c$, we have $I^2 \propto nK^2$. In the growth regime of the stochastic version, $I^2 \propto nK^2$, similar to the deterministic version with $K \gg K_c$.

Finally, let us discuss some open points. The first one concerns the link between the obtained scaling relations and the phase-space properties. It is clear that this link is beyond our present analysis. However, we can make some simple comments when $I_0 \ll K$. The scaling approach is useful to characterize the chaotic component. When $K \gtrsim K_c$, I^2 is constant for initial points inside the first island because the energy of each point is obviously limited. On the other hand, this average energy has a scaling behavior for points in the chaotic region. Then, the divergence of the crossover iteration number n_x can be associated with the breaking of the last spanning curve. For $K \gg K_c$, the n_x 'time scale' disappears because now the phase space is almost all open and we must have a new scaling function. The second point is related to the development of a renormalization group that can furnish the values of the exponents. Unfortunately, we do not know how to do it yet.

Acknowledgments

We thank Ronald Dickman for a critical reading of the manuscript. D G Ladeira was supported by Conselho Nacional de Desenvolvimento Científico (CNPq). J K L da Silva thanks Fundação de Amparo à Pesquisa (FAPEMIG) and CNPq, Brazilian agencies, for partial financial support.

References

[1] Fermi E 1949 *Phys. Rev.* **75** 1169
[2] Lichtenberg A J and Lieberman M A 1992 *Regular and Chaotic Dynamics (Appl. Math. Sci.* vol 38*)* (New York: Springer)
[3] Lieberman M A and Lichtenberg A J 1971 *Phys. Rev.* A **5** 1852
[4] Pustylnikov L D 1978 *Trans. Mosc. Math. Society* **2** 1
[5] Saif F 2005 *Phys. Rep.* **419** 207
Saif F 2006 *Phys. Rep.* **425** 369
[6] Lichtenberg A J, Lieberman M A and Cohen R H 1980 *Physica* D **1** 291
[7] Chirikov B V 1979 *Phys. Rep.* **52** 263
[8] Karner G 1994 *J. Stat. Phys.* **77** 867
[9] Dembinski S T, Makowski A J and Peplowski P 1993 *Phys. Rev. Lett.* **70** 1093
[10] José J V and Cordery R 1986 *Phys. Rev. Lett.* **56** 290
[11] Chen W-Y and Milburn G J 1997 *Phys. Rev.* E **56** 351
[12] Kowalik Z J, Franaszek M and Pieranski P 1988 *Phys. Rev.* A **37** 4016
[13] Warr S, Cooke W, Ball R C and Huntley J M 1996 *Physica* A **231** 551
[14] Leonel E D, Mcclintock P V E and da Silva J K L 2004 *Phys. Rev. Lett.* **93** 14101
[15] da Silva J K L, Ladeira D G, Leonel E D, McClintock P V E and Kamphorst S O 2006 *Braz. J. Phys.* **36** 700
[16] Ladeira D G and da Silva J K L 2006 *Phys. Rev.* E **73** 026201
[17] Leonel E D, da Silva J K L and Kamphorst S O 2004 *Physica* A **331** 435
[18] Leonel E D and Mcclintock P V E 2004 *J. Phys. A: Math. Gen.* **37** 8949
[19] Leonel E D and Mcclintock P V E 2005 *Chaos* **15** 33701
[20] Leonel E D 2007 *Phys. Rev. Lett.* **98** 114102
[21] Saif F and Rehman I 2007 *Phys. Rev.* A **75** 043610
[22] Hammersley J M 1961 *Proc. 4th Berkeley Symp. Math. Stat. Prob.* (Berkeley, CA: University of California Press) vol 3 p 79
[23] Karlis A K, Diakonos F K, Constantoudis V and Schmelcher P 2006 *Phys. Rev. Lett.* **97** 194102